

## Supplemental Methods

### Mice and Treatment

Tamoxifen (TAM) inducible *SclCre<sup>ER</sup>* mice <sup>1</sup> were crossed with Cre-recombinase inducible human *JAK2* mutant mice <sup>2,3</sup> to obtain *SclCre;JAK2-V617F (VF)* and *SclCre;JAK2 Exon12 (E12)* transgenic mice. All mice used in this study were on pure C57BL/6N background. Cre expression was induced by 2 mg of tamoxifen for 5 consecutive days. For dietary experiments, 2- to 3- months old mice were fed with normal chow diet (ND; D12450B, Research Diets) or HFD (D12492, Research Diets) for indicated time. For high glucose diet (HGD) feeding experiments mice were treated with ssniff® EF R/M High glucose pellets (Cat. E15629-34, ssniff® special diets, Germany) and supplemented with 15% glucose in water. For prolonged fasting, mice were fasted with alternate days of fasting-feeding cycles. Body weight of mice on normal chow diet (ND) or HFD was monitored every week.

### Body Composition Analysis

An EchoMRI-700 quantitative nuclear magnetic resonance analyzer (Echo Medical Systems) was used to measure the total fat and lean mass of chow diet fed mice. Data was expressed as the ratio of fat mass and lean mass to the total body mass.

### Comprehensive Laboratory Animal Monitoring System (CLAMS) Analysis

Comprehensive animal metabolic monitoring system (CLAMS; Columbus Instruments, Columbus, OH) was used to evaluate food consumption, locomotor activity, energy expenditure, oxygen consumption ( $VO_2$ ),  $CO_2$  production ( $VCO_2$ ) and respiratory exchange ratio (RER). RER is the ratio of  $VCO_2$  to  $VO_2$ , which changes depending on the energy source the animal are using. Locomotor activity was measured on X, Y and Z-axis by using infrared beams. Feeding was measured by recording the difference in the scale measurement of the center feeder from one time point to another. We studied mice for 2 light and 2 dark cycles after an acclimatization of 2 days.

### Flow Cytometry

Total BM cells were harvested from long bones (2 tibias and 2 femurs) by crushing bones with mortar and pestle using staining media (Dulbecco's PBS+ 5% FCS). Cells were filtered through 70 $\mu$ m nylon mesh to obtain a single-cell suspension. Red blood cells were depleted by treatment with erythrocyte lysis buffer (ACK buffer, Invitrogen). The following monoclonal

antibodies were used for FACS analysis and cell sorting: A mixture of biotinylated monoclonal antibodies CD3, CD4, CD8, CD19, B220, TER-119, Mac-1, and Gr-1 was used as the lineage mix (Lin). Anti-CD3e (17-A2), anti-CD4 (L3T4), anti-CD8 (53-6.72), anti-B220 (RA3-6B2), anti-TER-119, Gr-1 (RB6-8C5), anti-Mac-1 (M1/70), anti-CD105 (MJ7/18), anti-CD41 (MWRReg30), anti-APC-Kit (2B8), CD150 (TC15-12F12.2, all are from Biolegend); PE-Cy7- or PerCp5.5-anti-Sca-1 (E13-161.7), APC- or FITC-anti-CD34 (RAM34), anti-CD48 (HM48-1), PE-Cy7-CD127 (A7R34) (eBiosciences); PE-anti-Flt3 (A2F10.1), PE-Fc $\gamma$ RII/III (2.4G2) (Biolegend), biotinylated-leptin receptor antibody (BAF497; R&D Systems). Sytox-Blue (Invitrogen) was used to exclude dead cells during FACS analysis. Live, singlet cells were selected for gating and cell sorting. Cells were analyzed on a Fortessa Flow Cytometer and sorted on a FACSAria-II cell sorter (BD biosciences). Data were analyzed either using FACS Diva software or FlowJo (version 10.0.08) software (Treestar).

### **Bone marrow (BM) Transplantation Assays**

For competitive transplantation assays, erythrocyte depleted total bone marrow cells (BM) ( $1 \times 10^6$ ) from 8-12 week *VF* or *E12* transgenic mice or wildtype mice co-expressing GFP under UBC promoter were mixed with  $1 \times 10^6$  BM cells (1:1) from recipient type cells (competitor) and injected intravenously (in 200 $\mu$ l PBS/mouse) into lethally irradiated (1000rads) wildtype syngeneic (C57BL/6) recipient mice. Hematopoietic reconstitution was assessed in recipient peripheral blood (PB).

### **Determination of Mitochondrial Mass by Flow Cytometry**

For mitochondrial mass determination, total BM cells were incubated with 50nM of MitoTracker Green (Invitrogen) at 37°C for 20min after being stained with surface markers to identify indicated populations. Cells were washed twice in PBS, and then fluorescent intensity was measured by flow cytometry for MitoTracker Green in the FITC channel.

### **Determination of Mitochondrial DNA Copy Number**

Total DNA from indicated cell types was prepared using QIAamp DNA Mini Kit (Qiagen). Mitochondrial copy number was determined by measuring ratio of mitochondrial gene *Mito1* (for mouse) or *ND1* (for human) to the nuclear gene *Gusb* by quantitative real-time PCR.

### **Measurement of Intracellular ROS Levels by Flow Cytometry**

For measurement of cellular reactive oxygen species (ROS) levels, cells were incubated with the redox-sensitive probe 2',7'-dichlorodihydrofluorescein diacetate (CM-H<sub>2</sub>DCFDA; Invitrogen) (5 $\mu$ M) at 37°C for 30min. Cells were then washed once with PBS and resuspended in FACS staining buffer. Thereafter cells were stained with surface antibodies to define the stem and progenitor subsets as described above. Cells were then washed once with PBS, resuspended in FACS staining buffer and analyzed immediately by Fortessa flow cytometer for CM-H<sub>2</sub>DCFDA fluorescence in the FITC channel. For *in vitro* N-Acetyl L-Cysteine (NAC) treatment, 6-10 hours prior drug treatment cells were treated with NAC (1.5mM).

### **ELISA**

Mouse plasma leptin levels were measured by ELISA according to the suppliers guidelines (R&D systems). Serum insulin levels were measured by Ultra Sensitive Insulin Detection ELISA Kit (Crystal Chem).

**Glucose Tolerance Test (GTT).** Mice were fasted for 6h and injected i.p. with D-glucose (2g/kg of body weight). Blood samples were obtained by tail vein bleeding just before injection (time 0) and at 15, 30, 60, 90, and 120min post-D-glucose injection. Blood glucose was monitored with a glucometer (Abbott).

### **Glucose Uptake Assay.**

For measurement of glucose uptake, cells were starved for 4hrs in glucose free DMEM medium containing 1%BSA at 37°C. Cells were then loaded with or without 2-(n-(7-nitrobenz-2-oxa-1,3-diazol-4-yl)amino)-2-deoxyglucose (2-NBDglucose, 50 $\mu$ M, Invitrogen) for 30 minutes. Cells were washed twice in cold PBS and stained with surface markers to define stem and progenitor subsets as described above. Cells were analyzed by Fortessa flow cytometer for 2-NBD glucose fluorescence in the FITC channel.

### **Seahorse metabolic analyses**

Sorted lineage-negative, Sca-1<sup>+</sup> and cKit<sup>+</sup> (LSK) cells or megakaryocyte and erythroid progenitor (MEP) cells (10<sup>5</sup> cells per well) were cultured for 8 hours in serum free StemSpan medium (Stem Cell Technologies) with low concentrations of mTPO (10ng/ml) and mSCF (20ng/mL). Cells were washed with unbuffered medium and attached to the bottom of a XF96 Tissue Culture Plate (Agilent) coated with BD Cell-Tak Cell Adhesive. Extracellular acidification rate (ECAR), indicative of glycolysis, was measured using XF-Glycolysis stress

kit (Agilent) under basal conditions, in the presence of glucose (10mM), mitochondrial inhibitor oligomycin (2 $\mu$ M), and glycolytic inhibitor 2DG (50mM). For the measurement of OXPHOS, FACS sorted cells were cultured for 8hrs in serum free StemSpan medium and plated as described above. One hour before the measurement, cells were treated with control BSA (fatty acid free) or with palmitate as a fatty acid source (Seahorse Biosciences). Oxygen consumption rate (OCR), indicative of mitochondrial oxidative phosphorylation, was measured using the Seahorse XF96 instrument (Agilent). Respiration was measured under basal conditions, in the presence of the mitochondrial inhibitor Oligomycin (2 $\mu$ M), mitochondrial uncoupler FCCP (5 $\mu$ M), fatty acid uptake inhibitor, Etomoxir (20 $\mu$ M) and respiratory chain inhibitor Rotenone (1 $\mu$ M). Data were normalized to cell numbers.

### **Isolation of RNA**

Isolation of RNA from the adipose tissue was performed using RNeasy Plus Micro Kit (Qiagen) per manufacturer's instructions. Isolation of RNA from FACS sorted HSPC subsets were prepared using Picopure RNA isolation kit (Applied Biosystems). The quality and concentration of total RNA were determined on Agilent 2100 Bioanalyzer using the Eukaryote Total RNA Pico Assay. Samples with RNA Index number (RIN) higher than 7 were used for library preparation. RNA was reverse transcribed and cDNA amplified with SMART-Seq v2 or v4 (Takara). Libraries were prepared with Nextera XT (Illumina) according to manufacturer's instructions. Samples were pooled to equal molarity and run on the Fragment Analyzer for quality check and used for clustering on the NextSeq 500 instrument (Illumina). Samples were sequenced using the NextSeq 500 High Output kit 75-cycles (Illumina), and primary data analysis was performed with the Illumina RTA version 2.1.3 and bcl2fastq-2.16.0.10.

### **RNA Sequencing Analysis**

Reads were mapped against the mouse genome (version mm10; NCBI build 38) using the spliced-read aligner STAR.<sup>4</sup> All subsequent gene expression data analysis was done within the R software (R Foundation for Statistical Computing, Vienna, Austria). Raw reads and mapping quality was assessed by the qQCReport function from the R/Bioconductor software package QuasR.<sup>5</sup> Expression of RefSeq genes (annotation downloaded from UCSC 2015-12-18) was quantified by counting reads mapping into exons using the qCount function of QuasR. For gene expression visualization the resulting count table was normalized using function voom

from the R/Bioconductor software package limma, including a quantile normalization to adjust for library composition biases.<sup>6</sup> Subsequently, limma was used for detecting differentially expressed genes between genotypes. P-values for the contrasts between genotypes were calculated by likelihood ratio tests and adjusted for multiple testing by controlling the expected false discovery rate (Benjamini and Hochberg, 1995). Gene Set Enrichment Analysis was conducted using function camera of the limma package. Gene Sets were derived from MSigDB version 6.<sup>7</sup> Additionally, differentially expressed genes were analyzed using Ingenuity Pathway Analysis (IPA).

### **Metabolomics**

Metabolites of FACS purified bone marrow LSK and MEP cells were profiled using ultrahigh performance liquid chromatography–tandem mass spectrometry (UPLC–MS/MS) similar to a previously described protocol.<sup>8</sup> In brief, cells were lysed and extracted with 200 $\mu$ L MeOH/H<sub>2</sub>O (4:1 v:v) using bead type homogenizer. After centrifugation (15min at 13000rpm, at 4°C), the supernatant with soluble metabolites was collected and stored at –20°C. Prior to analysis, an aliquot of 100 $\mu$ L of the extracts were dried down under a stream of nitrogen and reconstituted in 20 $\mu$ L of water, further diluted with 80 $\mu$ L of 50mM ammonium acetate in acetonitrile/MeOH (90:9 v:v) adjusted with ammonium hydroxide to pH9. Metabolites were separated on nanoAquity UPLC (Waters) equipped with a BEH-Amide capillary column (200 $\mu$ m x150mm, 1.7 $\mu$ m particle size, Waters), Buffer A was 0.5mM ammonium acetate in acetonitrile (95%); buffer B was 0.5mM ammonium acetate in water; both buffers were adjusted with ammonium hydroxide to pH9. A gradient from 90% A to 50% A was applied. The injection volume was 1 $\mu$ L. The UPLC was coupled to a Synapt HDMS G2 mass spectrometer (Waters) by a nanoESI source. MS data was acquired using negative polarization and all ion fragmentation (MS<sup>E</sup>) over a mass range of 50 to 1200 m/z at a resolution of 22'000 (MS and MSMS). All solvents used were of quality HPLC grade (Chromasolv, Sigma-Aldrich). Metabolite data sets were evaluated with Progenesis QI software (Nonlinear Dynamics), which aligns the ion intensity maps based on a reference data set, followed by a peak picking on an aggregated ion intensity map. Detected ions were identified based on accurate mass, detected adduct patterns and isotope patterns by comparing with entries in the Human Metabolome Data Base (HMDB). A mass accuracy tolerance of 5mDa was set for the searches. Fragmentation patterns were considered for the identifications of metabolites. All biological samples were analyzed in triplicate; additionally, quality controls were used to

determine technical accuracy and stability. Altered concentrations of metabolites that were classified into groups using Metabolic Pathway Enrichment Analysis (MPEA) as previously described.<sup>9</sup>

### **Stable Isotope ([U-<sup>13</sup>C<sub>6</sub>] D-glucose) Labeling Studies**

FACS sorted LSK and MEP cells were cultured in SILAC DMEM Flex media (Cat#A24939-01) supplemented with 10% heat-inactivated dialyzed FBS (Sigma), mSCF (20ng/mL) mTPO (20ng/mL) and either 10mM U-13C6 D-Glucose (cat#CLM-1396-1, Cambridge Isotope Laboratories) or 10 mM glucose for 8 hours. Cells were washed twice in cold PBS and cell pellets were snap-frozen and stored at -80oC. The frozen cell pellets were processed and analyzed by IC-FTMS at Resource Center for Stable Resolved Metabolomics facility (RCSIRM) (<http://bioinformatics.cesb.uky.edu/bin/view/RCSIRM/WebHome>), University of Kentucky, USA.

### **Cell Fractionation**

The frozen cell pellets were homogenized in 60% cold CH<sub>3</sub>CN in a ball mill (Precellys- 24, Bertin Technologies) for denaturing proteins and optimizing extraction. Polar metabolites were extracted by the solvent partitioning method with a final CH<sub>3</sub>CN:H<sub>2</sub>O:CHCl<sub>3</sub> (2:1.5:1, v/v) ratio, and total protein extracted and quantified, as described previously (Sellers et al., 2015). The polar extracts were lyophilized before reconstitution in H<sub>2</sub>O for IC-Fourier Transform Mass Spectrometer (IC-FTMS) analysis.

### **Ion Chromatography - Fourier Transform Mass Spectrometry (IC-FTMS) Analysis**

Polar extracts were reconstituted in ultrapure deionized water (EMD Millipore) in a volume based on cell number. All analyses were performed on a Dionex ICS-5000+ ion chromatograph interfaced to a Thermo Fusion Orbitrap Tribrid mass spectrometer (IC-FTMS) (Thermo Fisher Scientific). Ion chromatography was performed using an IonPac AS11-HC-4 μm RFIC&HPIC (2×250 mm) column and an IonPac AG11-HC-4 μm guard column (2×50 mm). The column flow rate was kept at 0.38 mL/min with column temperature at 35°C and 0.06 mL/min methanol added post-column as a makeup solvent to aid vaporization in the heated electrospray ionization (HESI) unit. The HESI vaporizer temperature was 400°C with sheath gas set at 35 Arb and auxiliary nitrogen flow at 4 Arb. The column was initially equilibrated for 8 min with 1mM KOH, and then followed by 1mM KOH for 2 min after 10μL of sample was injected. The KOH gradient program used to elute samples included ramping up

to 40 mM KOH from 2 to 25min, and to 100m Mfrom25 to 39.1 min, at 100 mM to 50min, and ramping down to 1mM KOH at 50.1 min and at 1mM KOH to 52.5 min. KOH suppression was achieved with a Dionex AERS 500 2 mm suppressor with an external AXP pump supplying regenerant at a flow rate of 0.75 mL/min and injected into the Orbitrap mass spectrometer via HESI. Mass spectra were recorded at a resolution of 450,000 (achieving a resolution of  $\sim 360'000$  at 400 m/z) from 80 to 700 m/z mass scan range, with detection in the negative ion mode voltage using the following settings: HESI = 2800 V; ion transfer tube temperature = 300°C; automatic gain control (AGC) =  $2 \times 10^5$ ; maximal injection time = 100 msec. Peak areas were integrated and exported to Excel via the Thermo TraceFinder (version 3.3) software package. Peak areas were corrected for natural abundance as previously described (Moseley, 2010). The number of moles of each metabolite was determined by calibrating the natural abundance-corrected signal against that of authentic external standards. The amount was normalized to the amount of extracted protein, and is reported in  $\mu\text{mol/g}$  protein.

### **Protein Expression Measurement**

Indicated cell types were fixed in a fixation buffer for 30 minutes at 4°C. Cells were washed twice with the permeabilization wash buffer (BD bioscience) and incubated with rabbit anti-PFKFB3 antibody (1:100 dilution) (Cell Signaling Technology, Clone:D7H4Q; Cat#13123S) for 2hours at 4°C. Cells were washed twice with permeabilization wash buffer and then incubated with Goat anti-Rabbit IgG (H+L)–APC conjugated antibody (1:400 dilution) for one hour. Cells were washed twice and resuspended in FACS buffer. Mean fluorescence intensity of PFKFB3 in APC channel was measured by FACS.

### **GSH/GSSG and NADPH Measurement**

GSH/GSSG ratio was measured using GSH/GSSG-Glo Assay (Promega) according to the supplier's instructions. NADPH levels were measured using NADP/NADPH calorimetric assay kit (Cat# MAK038-1KT, Sigma). For both assays, cells were treated with indicated concentrations of 3PO or Ruxolitinib alone or in combination for 24 hours. For NAC treatment, cells were pretreated with 1.5mM NAC for 6hours. Data are normalized to untreated controls.

### **Histology**

Indicated tissues were fixed in 4% PFA overnight and subjected to standard H&E staining procedures. Pictures were taken using Leica DM 2000 microscope.

### **Adipocyte Size Determination**

Epididymal fat tissues were fixed in 4% formalin for over night. Fixed issues were embedded in paraffin and thin sections were stained with hematoxylin and eosin staining. Adipocyte size was determined with NIH CellProfiler software 2.1.1 (<http://cellprofiler.org/>) by measuring 100 cells per image, and four to five images were analyzed per slide.

### **Transmission Electron Microscopy**

FACS sorted BM HSPCs were pooled from identical genotypes ( $10^5$  cells per genotype). Cells were fixed overnight in 2.5% glutaraldehyde at 4°C. Cells were pelleted at 3,000g for 10 min at 4°C. Cells were then submitted to the Biozentrum Electron Microscope Facility, Basel, for standard transmission electron microscopy ultrastructural analyses. Processed cells were imaged with AMT camera system with direct magnification of 4800x. Scale bar represents 500nm. Data are representative of >50 scanned cells per genotype.

### **Pharmacological inhibitors treatment *in vivo* and *in vitro***

Ruxolitinib treatment (60-90mg/kg; daily oral gavage) was performed as previously described.<sup>10</sup> 3PO (3-(3-pyridinyl)-1-(4-pyridinyl)-2-propen-1-one; Axon Medchem, 2175) was dissolved in DMSO to make a stock solution. Stock was dissolved in warm saline solution and administered immediately (50mg/kg, daily) by intraperitoneal (i.p) injection for indicated time. In experiments testing 3PO efficacy on MPN progression, treatment was initiated at 6 weeks post-TAM induction (for *VF*) or 2-weeks post-TAM induction (for *E12*). In experiments testing 3PO efficacy on MPN initiation, treatment was initiated immediately after TAM induction for indicated time. Human myeloid leukemia cell lines SET2, HEL, UKE1 (*JAK2-V617F* positive) and K562 cells (*JAK2-V617F* negative and *BCR-ABL* positive) were cultured in RPMI-1640 medium supplemented with 20% FCS. For *in vitro* pharmacological inhibition experiments, cells were treated with 10-30 $\mu$ M of 3PO or 250nM of Ruxolitinib for indicated time. For NAC treatment, 6 hours prior drug treatment cells were pretreated with NAC (1.5mM).

### **Statistical Analyses**

Statistical analysis was performed with the use of two-tailed Student's unpaired t-test analysis (when the statistical significance of differences between two samples was assessed) or one-way ANOVA analyses followed by Tukey's multiple comparison tests were used for multiple group comparisons (when the statistical significance of differences between more than two groups was assessed), or two-way ANOVAs with subsequent Holm-Sidak's multiple comparison tests with alpha 0.05 as significant (when comparing between groups; for hematopoietic recovery analysis) with Prism software version 7.0 (GraphPad Inc). Survival rate in mouse experiments was represented with Kaplan-Meier curves and significance was estimated with the log-rank test (Prism GraphPad). Significance is denoted with asterisks (\* $p < 0.05$ , \*\* $p < 0.01$ , \*\*\* $p < 0.001$ ).

### Data Availability

The RNAseq data have been submitted to the Gene Expression Omnibus under accession number GSE 116571.

For detailed information on resources and reagents used in this study see Supplemental Data.

Requests for resources and reagents should be directed to, Radek C. Skoda (radek.skoda@unibas.ch).

### References

1. Gothert JR, Gustin SE, Hall MA, et al. In vivo fate-tracing studies using the Scl stem cell enhancer: embryonic hematopoietic stem cells significantly contribute to adult hematopoiesis. *Blood*. 2005;105(7):2724-2732.
2. Tiedt R, Hao-Shen H, Sobas MA, et al. Ratio of mutant JAK2-V617F to wild-type Jak2 determines the MPD phenotypes in transgenic mice. *Blood*. 2008;111(8):3931-3940.
3. Grisouard J, Li S, Kubovcakova L, et al. JAK2 exon 12 mutant mice display isolated erythrocytosis and changes in iron metabolism favoring increased erythropoiesis. *Blood*. 2016;128(6):839-851.
4. Dobin A, Davis CA, Schlesinger F, et al. STAR: ultrafast universal RNA-seq aligner. *Bioinformatics*. 2013;29(1):15-21.
5. Gaidatzis D, Lerch A, Hahne F, Stadler MB. QuasR: quantification and annotation of short reads in R. *Bioinformatics*. 2015;31(7):1130-1132.
6. Law CW, Chen YS, Shi W, Smyth GK. voom: precision weights unlock linear model analysis tools for RNA-seq read counts. *Genome Biology*. 2014;15(2).
7. Liberzon A, Birger C, Thorvaldsdottir H, Ghandi M, Mesirov JP, Tamayo P. The Molecular Signatures Database (MSigDB) hallmark gene set collection. *Cell Syst*. 2015;1(6):417-425.

8. Valdivieso P, Vaughan D, Laczko E, et al. The Metabolic Response of Skeletal Muscle to Endurance Exercise Is Modified by the ACE-I/D Gene Polymorphism and Training State. *Front Physiol.* 2017;8:993.
9. Xia J, Wishart DS. Using MetaboAnalyst 3.0 for Comprehensive Metabolomics Data Analysis. *Curr Protoc Bioinformatics.* 2016;55:14 10 11-14 10 91.
10. Kubovcakova L, Lundberg P, Grisouard J, et al. Differential effects of hydroxyurea and INC424 on mutant allele burden and myeloproliferative phenotype in a JAK2-V617F polycythemia vera mouse model. *Blood.* 2013;121(7):1188-1199.

**Supplemental Table 1.** Antibodies used in this study

<b>Antibodies</b>	<b>Source</b>	<b>Identifier</b>
Biotinylated anti-mouse CD3e (17-A2)	Biologend	Cat. # 100244, RRID AB_2563947
Biotinylated anti-mouse CD4 (L3T4)	Biologend	Cat. # 100404, RRID AB_312689
Biotinylated anti-mouse CD8 (53-6.7)	Biologend	Cat. # 100704, RRID AB_312743
Biotinylated anti-mouse CD19 (6D5)	Biologend	Cat. # 115504, RRID AB_313639
Biotinylated anti-mouse B220 (RA3-6B2)	Biologend	Cat. # 103204, RRID AB_312989
Biotinylated anti-mouse TER-119	Biologend	Cat. # 116204, AB_313705
Biotinylated anti-mouse Mac-1 (M1/70)	Biologend	Cat. # 101204, RRID AB_312787
Biotinylated anti-mouse Gr-1 (RB6-8C5)	Biologend	Cat. # 108404, RRID AB_313369
APC anti-mouse CD105 (MJ7/18)	Biologend	Cat. # 120414, RRID AB_2277914
BV 605 anti-mouse CD41 (MWReg30)	Biologend	Cat. # 133921, RRID AB_2563933
APC anti-mouse cKit (2B8)	Biologend	Cat. # 105812, RRID AB_313221
PE anti-mouse CD150 (TC15-12F12.2)	Biologend	Cat. # 115904, RRID AB_313683
PE-Cy7 anti-mouse CD150 (TC15-12F12.2)	Biologend	Cat. # 115914, RRID AB_439797
PE-Cy7 anti-mouse Sca-1 (E13-161.7)	eBiosciences	Cat. # 25-5981-82, RRID AB_469669
PerCp5.5 anti-mouse Sca-1 (E13-161.7)	eBiosciences	Cat. # 45-5981-82, RRID AB_914372
AF647 anti-mouse CD34 (RAM34)	BD Biosciences	Cat. # 560230
FITC anti-mouse CD34 (RAM34)	eBiosciences	Cat. # 11-0341-82, RRID AB_465021
FITC anti-mouse CD48 (HM48-1)	eBiosciences	Cat. # 11-0481-81 RRID 465076
PE-Cy7 anti-mouse CD127 (A7R34)	eBiosciences	Cat. # 25-1271-82, RRID AB_469649
PE anti-mouse Flt3 (A2F10)	Biologend	Cat. # 135306, RRID AB_1877217
PE anti-mouse FcγRII/III (2.4G2)	Biologend	Cat. # 101308, RRID AB_312807
FITC anti-Ki-67	BD Biosciences	Cat. # 558616
FITC anti-Annexin V	Biologend	Cat. # 640906
APC Goat anti-Rabbit IgG (H+L)	ThermoFisher Scientific	Cat. #A-21245
Streptavidin Pacific Blue conjugate	ThermoFisher Scientific	Cat. # S11222
anti-PFKFB3 antibody (D7H4Q)	Cell Signaling Technology	Cat. # 13123S

**Supplemental Table 2.** Human leukemia cells lines used in this study.

<b>Experimental models: cell lines</b>		
SET-2	ATCC	Cat# ACC608, RRID:CVCL 2187
HEL		N/A
UKE-1		N/A
K562		N/A

**Supplemental Table 3.** Details of mouse strains and mouse diets used in this study.

<b>Experimental models: mouse strains</b>		
BL57/6N	Janvier labs	Cat# 000664
<i>Scf-Cre;JAK2-V617F</i>	Kubovcakova L et al., 2013	N/A
<i>ScfCre; Exon 12</i>	Grisouard J et al., 2016	N/A
<i>ScfCre;Jak2-KI</i>	Hasan S et al., 2013	N/A
<i>ScfCre;JAK2-KI</i>	(24)	N/A
<i>VavCre;JAK2-V617F</i>	Tiedt R et al., 2008	N/A
<i>Stella Cre;JAK2-KI</i> heterozygous	(25)	N/A
<i>Stella Cre;JAK2-KI</i> homozygous	(25)	N/A
<i>Tg6</i>	(27)	N/A
<b>Mouse diets</b>		
Normal diet	Research Diets	Cat. # D12450B
High fat diet	Research Diets	Cat. # D12492
ssniff® EF R/M High glucose pellets	ssniff® special diets	Cat. # E15629-34

**Supplemental Table 4.** List of other reagents used in this study.

<b>Commercial Kits</b>		
RNeasy Plus Micro Kit	Quiagen	Cat. # 74034
Picopure RNA isolation kit	Applied Biosystems	Cat. # KIT0214
QIAamp DNA Mini kit	Quiagen	Cat. # 51306
PicoPure RNA Isolation Kit	Life Technologies	Cat. # KIT0204
GSH/GSSG-Glo™ Assay	Promega	Cat. # V6611
NADP/NADPH	Sigma	Cat. # MAK038-1KT
Ultra Sensitive Insulin Detection ELISA Kit	Crystal Chem	Cat. # 9080
Mouse Leptin DuoSet ELISA kit	R&D Systems	Cat. # DY498
RNA library preparation	Illumina	Cat.#RS-122-2001
Seahorse XF Glycolysis Stress Test Kit	Agilent	Cat. # 103020-100
Seahorse XF Mito Stress Test Kit	Agilent	Cat. # 103015-100
<b>Chemicals for flow cytometry</b>		
MitoTracker Green	Invitrogen	Cat. # M7514
CM-H <sub>2</sub> DCFDA	Invitrogen	Cat. # C6827
Sytox Blue	Invitrogen	Cat. # S34857
2-NBDG	Invitrogen	Cat. # N13195
Fixation buffer	BD Sciences	Cat. # 554655
Permeabilization solution	BD Sciences	Cat. # 347692

**Supplemental Table 5.** Cell culture reagents and pharmacological inhibitors used in this study.

<b>Cell culture reagents and additives</b>		
RPMI 1640	Gibco	Cat. # 21875091
Penicillin-Streptomycin	Gibco	Cat. # 15140130
FBS	Sigma	Cat. # F4135
StemSpan	Stem Cell Technologies	Cat. # 09650
BD Cell-Tak Adhesive	BD Sciences	Cat. # 354240
Recombinant mouse TPO	Peprotech	Cat. # 315-14
Recombinant mouse SCF	Peprotech	Cat. # 250-03
N-Acetyl-L-Cysteine	Sigma	Cat. # A9165
SILAC DMEM Flex media	Gibco	Cat. #A24939-01
U- <sup>13</sup> C <sub>6</sub> D-Glucose	Cambridge Isotope Laboratories	Cat. # CLM-1396-1
<b>Pharmacological inhibitors</b>		
Ruxolitinib	Novartis	N/A
3PO	Axon MedChem	Cat. # Axon 2175

**Supplemental Table 6.** List of primer sequences used for qRT-PCR analysis.

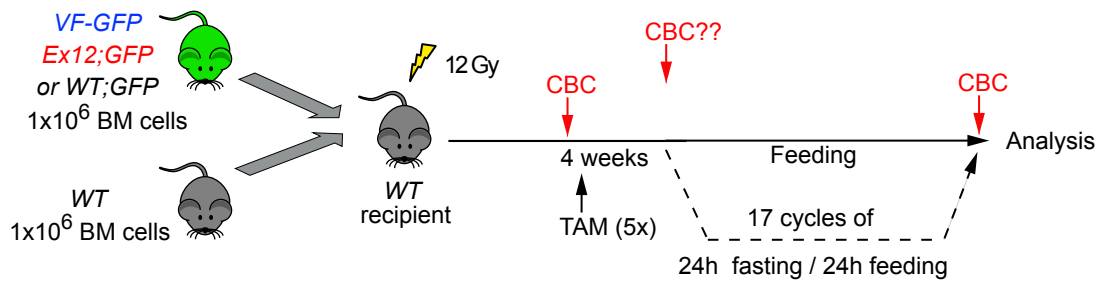
<b>Oligonucleotides</b>		
<i>IL-1<math>\alpha</math>-F</i>	CCATAACCCATGATCTGGAAGAG	Eurogentec
<i>IL-1<math>\alpha</math>-R</i>	GCTTCATCAGTTTGTATCTCAAATCAC	Eurogentec
<i>IL-1<math>\beta</math>-F</i>	CTCGTGGTGTCCGACCCATATGA	Eurogentec
<i>IL-1<math>\beta</math>-R</i>	TGAGGCCCAAGGCCACAGGT	Eurogentec
<i>Cxcl1-F</i>	GCTGGGATTCACCTCAAGAAC	Eurogentec
<i>Cxcl1-R</i>	AGCAGTCTGTCTTCTTTCTCC	Eurogentec
<i>Cxcl2-F</i>	TGTCAATGCCTGAAGACCC	Eurogentec
<i>Cxcl2-R</i>	CTCTTTGGTTCTTCCGTTGAG	Eurogentec
<i>Cxcl3-F</i>	CCGCGTTCTTCCATTTGTGT	Eurogentec
<i>Cxcl3-R</i>	GGTCATCTTGTGCGACATGATT	Eurogentec
<i>IL-6-F</i>	CTCTGCAAGAGACTTCCATCC	Eurogentec
<i>IL-6-R</i>	AGTCTCCTCTCCGGACTTGT	Eurogentec
<i>TNF-<math>\alpha</math>-F</i>	CAGCCGATGGGTTGTACCTT	Eurogentec
<i>TNF-<math>\alpha</math>-R</i>	GGCAGCCTTGTGCCTTGA	Eurogentec
<i>IL-10-F</i>	GTGAAGACTTTCTTTCAAACAAAG	Eurogentec
<i>IL-10-R</i>	CTGCTCCACTGCCTTGCTCTTATT	Eurogentec
<i>Mcp-1-F</i>	CCAGCACCAGCACCAGCCAA	Eurogentec
<i>Mcp-1-R</i>	TGGATGCTCCAGCCGGAAC	Eurogentec
<i>Mip1a-F</i>	CCCAGCCAGGTGTCATTTTCC	Eurogentec
<i>Mip1a-R</i>	GCATTTCAGTTCCAGGTCAGTG	Eurogentec
<i>Atgl-F</i>	GCCATGATGGTGCCTATACT	Eurogentec
<i>Atgl-R</i>	TCTTGGCCCTCATCACCAGAT	Eurogentec
<i>CD36-F</i>	CCTTGGCAACCAACCACAAA	Eurogentec
<i>CD36-R</i>	ATCCACCAGTTGCTCCACAC	Eurogentec
<i>Lpl-F</i>	TGCCGCTGTTTTGTTTTACC	Eurogentec
<i>Lpl-R</i>	TCACAGTTTCTGCTCCAGC	Eurogentec
<i>Fabp4-F</i>	CTGGTACATGTGCAGAAATGG	Eurogentec
<i>Fabp4-R</i>	GAAGTTCAGTCCAGGTCAACG	Eurogentec
<i>Hsl-F</i>	AGCCTCATGGACCTCTTCTA	Eurogentec
<i>Hsl-R</i>	TCTGCCTCTGTCCCTGAATAG	Eurogentec
<i>Mgll-F</i>	CTTGCTGCCAAACTGCTCAA	Eurogentec
<i>Mgll-R</i>	GGTCAACCTCCGACTTGTTC	Eurogentec
<i>Plin1-F</i>	TGCTGCACGTGGAGAGTAAG	Eurogentec
<i>Plin1-R</i>	TGGGCTTCTTTGGTGTCTGTT	Eurogentec
<i>Cideac (Cide-c)-F</i>	TCCAAGCCCTGGCAAAAGAT	Eurogentec
<i>Cideac (Cide-c)-R</i>	CGGAG-CATCTCCTTACGAT	Eurogentec
<i>Cpt1-F</i>	CACGCCATGATCATGTATCG	Eurogentec
<i>Cpt1-R</i>	ACATCCTCTCCATCTGGTAG	Eurogentec
<i>Fasn-F</i>	GTGATAGCCGGTATGTCCGGG	Eurogentec
<i>Fasn-R</i>	TAGAGCCCAGCCTTCCATCT	Eurogentec
<i>Ppary-F</i>	CCCACCAACTTCGGAATCAG	Eurogentec
<i>Ppary-R</i>	AATGCGAGTGGTCTTCCATCA	Eurogentec
<i>b-Actin-F</i>	TCACCCACACTGTGCCCATCTACGA	Eurogentec
<i>b-Actin-R</i>	GGATGCCACAGGATTCCATACCCA	Eurogentec
<i>mMito1-F</i>	CTAGAAACCCCGAAACAAA	Eurogentec
<i>mMito1-R</i>	CCAGCTATACCAAGCTCGT	Eurogentec
<i>GUSB-F-F</i>	TCTCCTTGTGTCTGCAGTGG	Eurogentec
<i>GUSB-R-R</i>	AGCCTCAAAGGGGAGGTG	Eurogentec
<i>ND-1-F</i>	TTCTAATCGCAATGGCATTCTT	Eurogentec
<i>ND-1-R</i>	AAGGGTTGTAGTAGCCCGTAG	Eurogentec

**Supplemental Table 7.** Software used in this study.

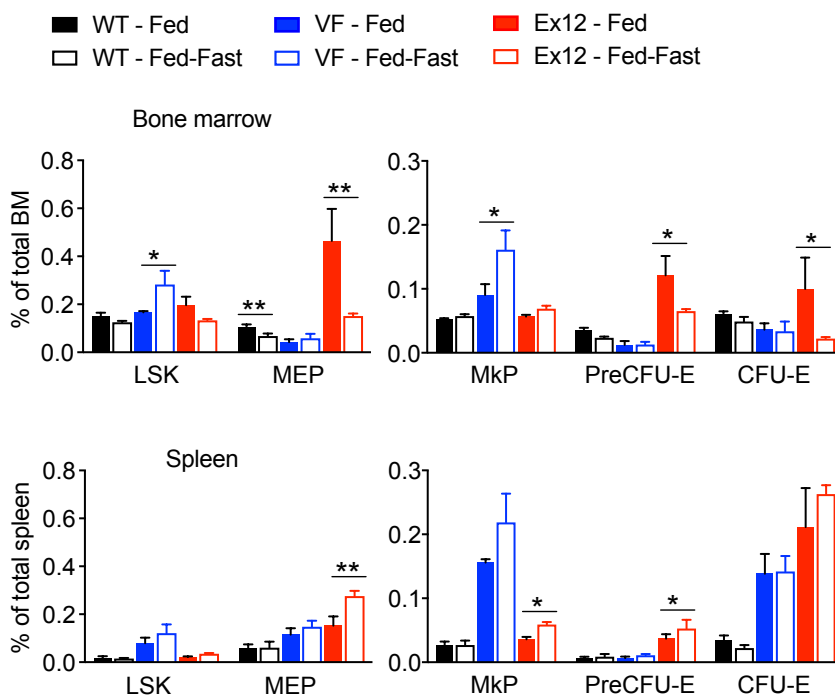
<b>Software and Algorithms</b>		
PRISM (version 6)	<a href="http://www.graphpad.com">www.graphpad.com</a>	GraphPad
FlowJo (version 9.8.2)	<a href="https://www.flowjo.com/">https://www.flowjo.com/</a>	N/A
R (version 3.4.2)	<a href="https://cran.r-project.org">https://cran.r-project.org</a>	N/A
bedtools	<a href="http://bedtools.readthedocs.io/en/latest/">http://bedtools.readthedocs.io/en/latest/</a>	N/A
samtools	<a href="http://samtools.sourceforge.net/">http://samtools.sourceforge.net/</a>	N/A
STAR aligner (version 2.6.0c)	<a href="https://github.com/alexdobin/STAR">https://github.com/alexdobin/STAR</a>	N/A
GSEA (version 2-2.1.0)	<a href="http://software.broadinstitute.org/gsea/index.jsp">http://software.broadinstitute.org/gsea/index.jsp</a>	N/A
Homer	<a href="http://homer.ucsd.edu/homer/index.html">homer.ucsd.edu/homer/index.html</a>	N/A
FastQC	<a href="https://www.bioinformatics.babraham.ac.uk/projects/fastqc/">https://www.bioinformatics.babraham.ac.uk/projects/fastqc/</a>	N/A
Progenesis QI software	<a href="http://www.nonlinear.com/progenesis/qi/">http://www.nonlinear.com/progenesis/qi/</a>	N/A
RCSIRM	<a href="http://bioinformatics.cesb.uky.edu/bin/view/RCSIRM/WebHome">http://bioinformatics.cesb.uky.edu/bin/view/RCSIRM/WebHome</a>	N/A
NIH CellProfiler software 2.1.1	<a href="http://cellprofiler.org/">http://cellprofiler.org/</a>	N/A
Metabolic Pathway Enrichment Analysis (MPEA)	<a href="http://www.metaboanalyst.ca/">http://www.metaboanalyst.ca/</a>	N/A

## Supplemental Figure S1

### A Schematic of intermittent fasting-feeding treatment

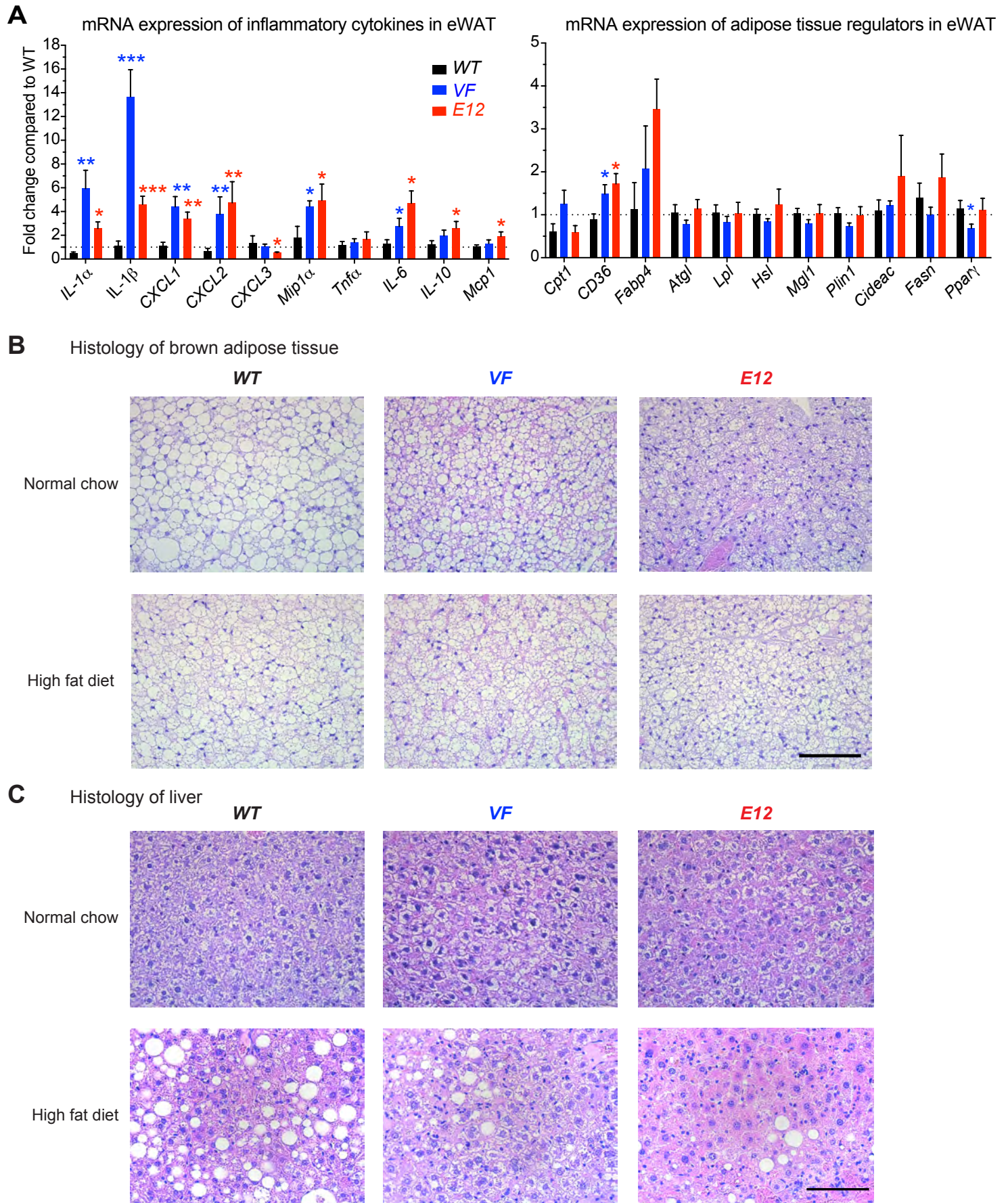


### B HSPC frequencies in bone marrow and spleen after 5 weeks of intermittent fasting-feeding treatment



**Supplemental Figure S1.** Reducing energy supply through fasting has beneficial effects in reducing MPN progression in MPN mice. (A) MPN induction and prolonged fasting scheme. Bone marrow transplant recipient mice were treated with tamoxifen (TAM) to activate the JAK2-VF and JAK2-E12 mutations. Four weeks after TAM injections, mice were fed normally or subjected to fasting with 17 cycles of 1d-fasting/1d-feeding regimen. (B) Bar graphs showing the frequency of donor derived HSPCs and megakaryocyte and erythroid committed progenitors in BM (upper panel) and spleen (lower panel) of indicated mice (n=4-5 mice per genotype). All data are presented as mean  $\pm$  SEM. One-way ANOVA analyses followed by Tukey's multiple comparison tests were used. \*P < .05; \*\*P < .01.

## Supplemental Figure S2

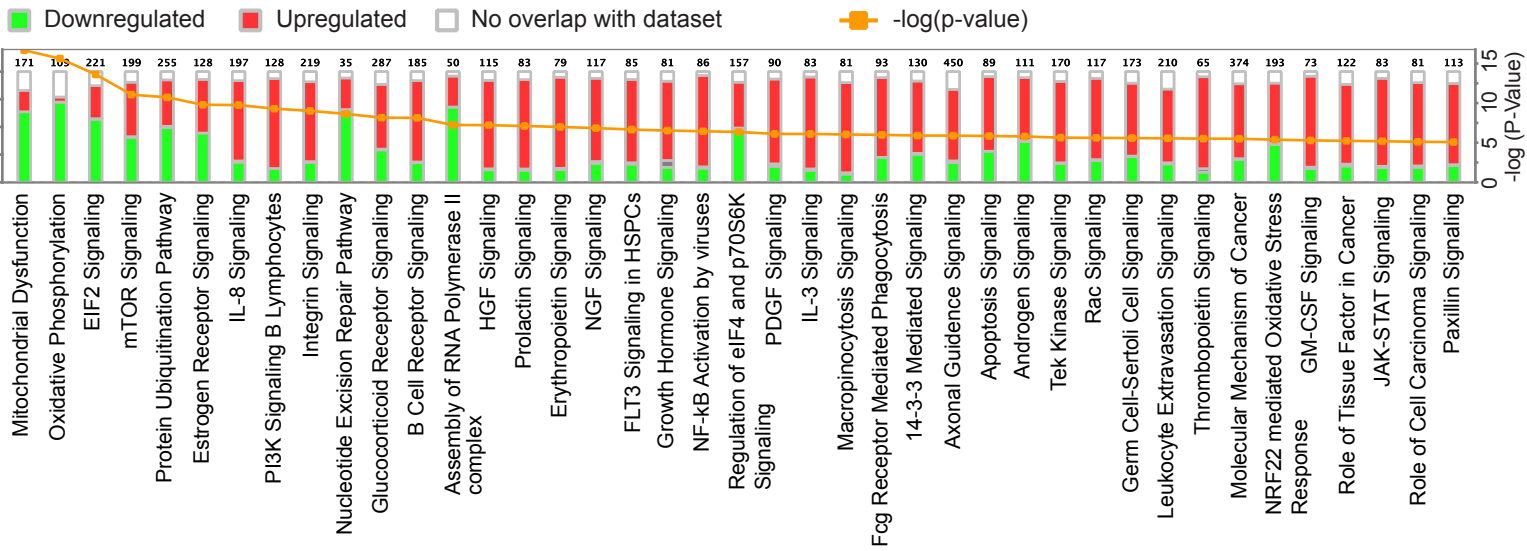


**Supplemental Figure S2:** A) Quantitative RT-PCR analyses of inflammatory cytokines (left) and adipose tissue regulators mRNA expression in eWAT (n= 5-6 mice per genotype). (B and C) Representative images of hematoxylin and eosin (H&E) staining of brown adipose tissue (B) and liver (C) from normal chow or high fat diet treated mice (n= 4-5 mice per genotype and treatment). Scale bars=100µm. All data are presented as mean ± SEM. One-way ANOVA analyses followed by Tukey's multiple comparison tests were used for multiple group comparisons. \*P < .05; \*\*P < .01; \*\*\*P < .001.

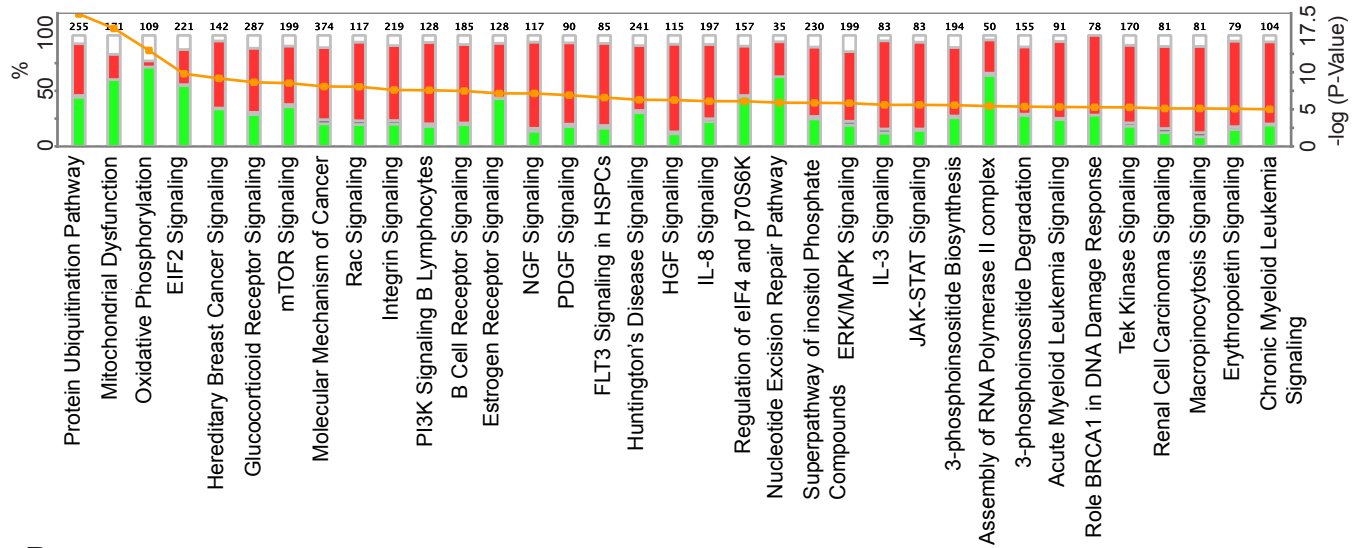
**Supplemental Figure S3.** Differentially expressed molecular pathways in bone marrow MEP cells expressing mutant JAK2. (A) Ingenuity pathway analysis (IPA) of differentially expressed genes in MEPs from VF (upper panel) and E12 (lower panel) compared to WT mice. (B) Competitive gene set enrichment pathway analysis (GSEA) of differentially expressed molecular pathways from the MSigDB hallmark gene sets in MEPs from VF (left panel) and E12 (right panel) compared to WT mice. (n=3 mice per genotype and cell type).

**A** Differentially regulated pathways in MEP cells by Ingenuity Pathway Analysis (IPA)

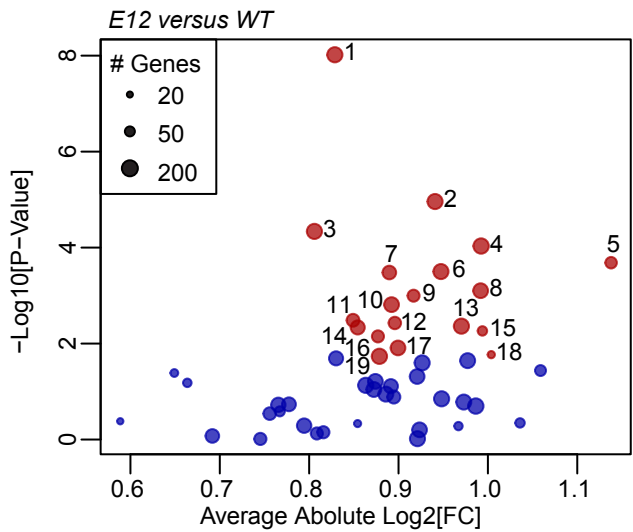
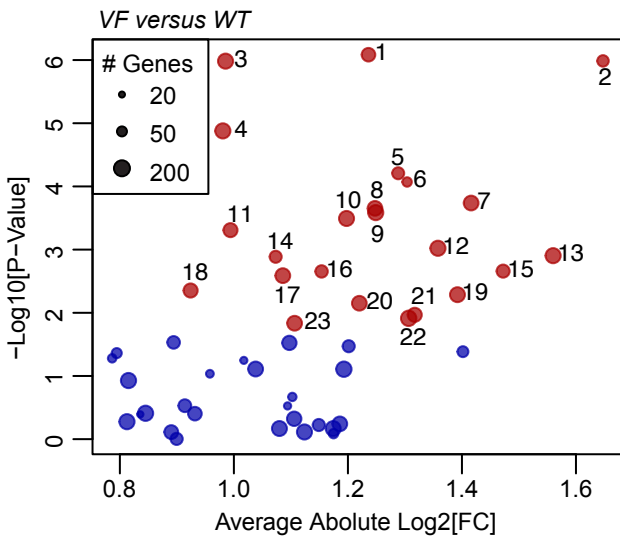
VF mice compared to wildtype controls



E12 mice compared to wildtype controls



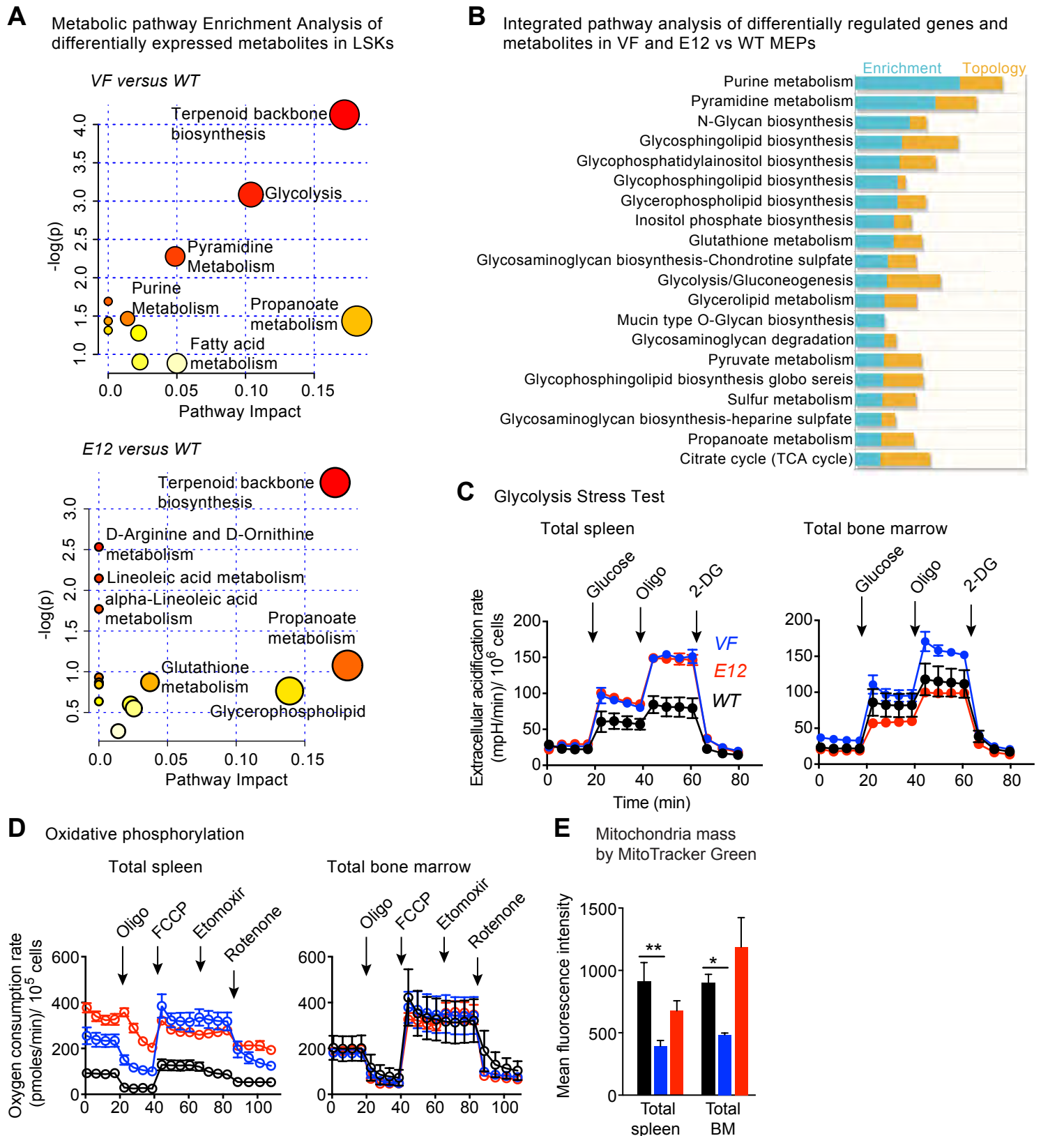
**B** Gene Set Enrichment Analysis (GSEA)



- |                             |                            |
|-----------------------------|----------------------------|
| 1 UV response down          | 13 Heme Metabolism         |
| 2 IL6 JAK STAT3 Signaling   | 14 Protein Secretion       |
| 3 Oxidative Phosphorylation | 15 Coagulation             |
| 4 Mitotic Spindle           | 16 PI3K AKT mTOR Signaling |
| 5 Androgen Response         | 17 Estrogen Response early |
| 6 TGF Beta Signaling        | 18 Fatty Acid Metabolism   |
| 7 Inflammatory Response     | 19 Hypoxia                 |
| 8 Apical Junction           | 20 Complement              |
| 9 Allograft rejection       | 21 Apoptosis               |
| 10 TNFα Signaling via NFκB  | 22 Interferon γ Response   |
| 11 DNA Repair               | 23 Kras Signaling up       |
| 12 IL2 STAT5 Signaling      |                            |

- |                             |                              |
|-----------------------------|------------------------------|
| 1 Mitotic Spindle           | 11 Unfolded Protein Response |
| 2 Oxidative Phosphorylation | 12 PI3K AKT mTOR Signaling   |
| 3 G2M Checkpoint            | 13 IL2 STAT5 Signaling       |
| 4 mTORC1 Signaling          | 14 DNA Repair                |
| 5 IL6 JAK STAT3 Signaling   | 15 TGF Beta Signaling        |
| 6 TNFα Signaling Via NFκB   | 16 Protein Secretion         |
| 7 UV Response down          | 17 Apical Junction           |
| 8 Inflammatory Response     | 18 Notch Signaling           |
| 9 Androgen Response         | 19 E2F Targets               |
| 10 Estrogen Response early  |                              |

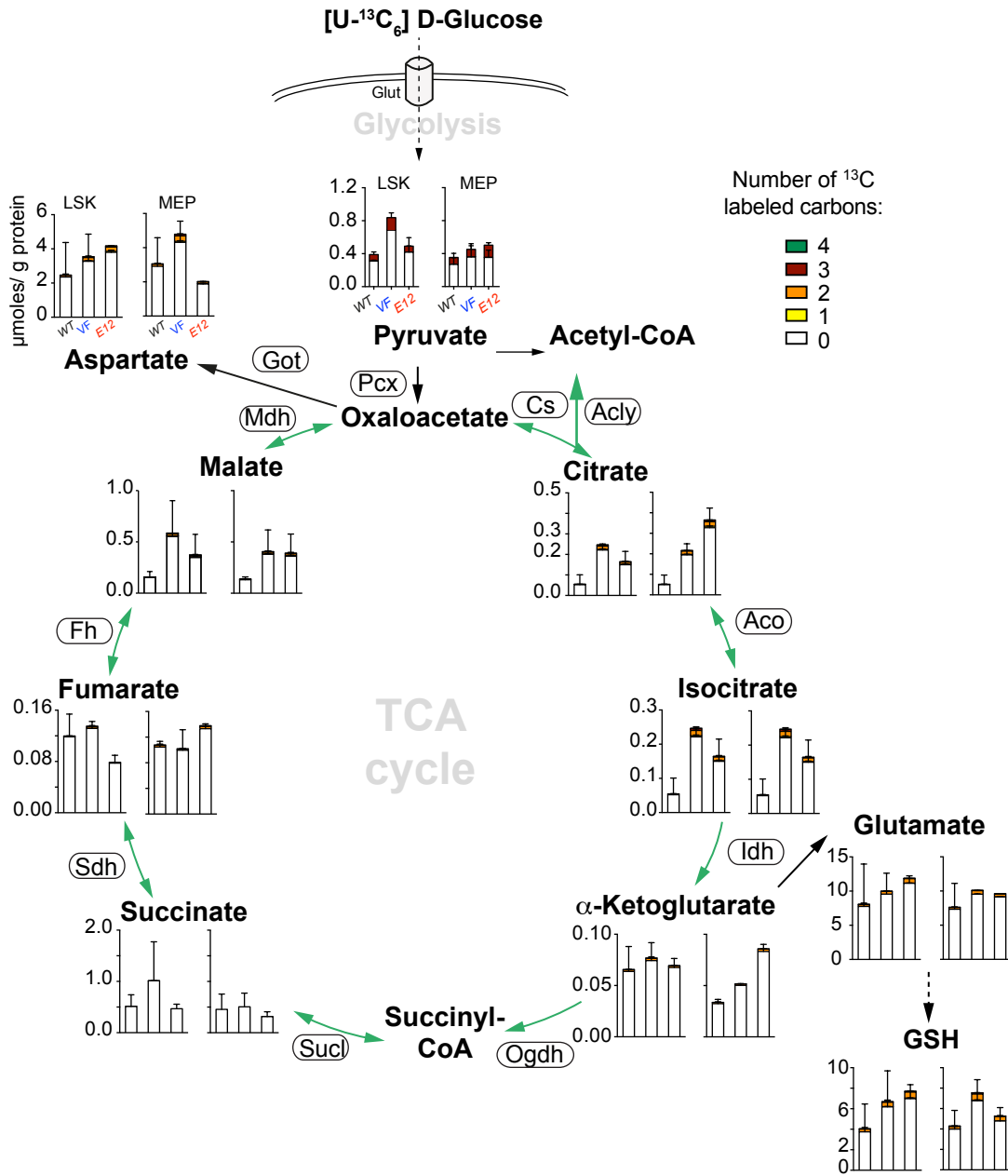
## Supplemental Figure S4



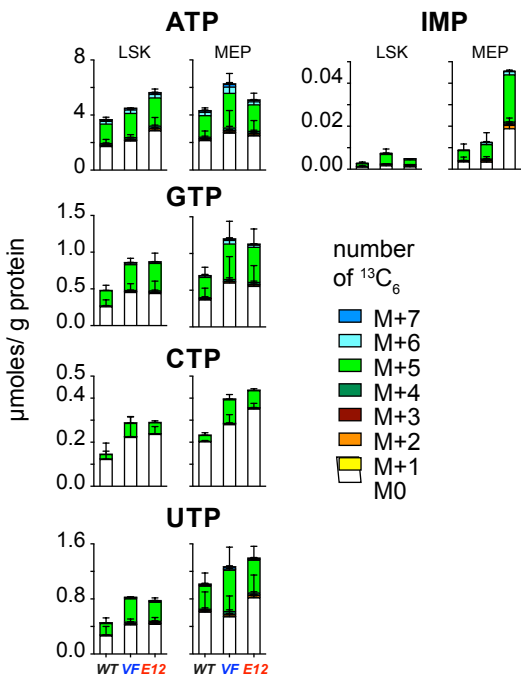
**Supplemental Figure S4:** Transcriptomic and metabolomic profiles of mutant JAK2 expressing hematopoietic stem and progenitor cells unveiled altered metabolic regulators. (A) Metabolic pathway enrichment analysis of significantly up-regulated metabolites in bone marrow MEPs from VF (upper panel) and E12 (lower panel) compared to WT mice as determined by MetaboloAnalyst 3.0 (n=3 per genotype). (B) Integrated pathway analysis of differentially regulated genes and metabolites in MEP cells from VF and E12 compared to WT mice. (C) Measurements of glycolytic rates from total spleen (left graph) and bone marrow cells (right graph). Extracellular acidification rate (ECAR) values were normalized to cell numbers. Data are from 3 independent experiments (n=6 mice per genotype). (D) Measurements of oxygen consumption rate (OCR), indicative of mitochondrial oxidative phosphorylation from total spleen (left graph) and bone marrow cells (right graph). OCR values were normalized to cell numbers. Data are from 3 independent experiments, n=6 mice per genotype. (E) Mitochondrial abundance as determined by the mean fluorescence intensity of MitoTrackerGreen in total spleen and bone marrow cells (n=5 mice per genotype). All data are presented as mean  $\pm$  SEM. One-way ANOVA analyses followed by Tukey's multiple comparison tests were used for multiple group comparisons. \*P < .05; \*\*P < .01; \*\*\*P < .001.

**Supplemental Figure S5.** Metabolic tracing of [ $^{13}\text{C}_6$ ] D-glucose of glucose in TCA cycle and nucleotides in mutant *JAK2* expressing hematopoietic stem and progenitor cells. (A) Bar graphs depicting the levels ( $\mu\text{moles per gram protein}$ ) of glucose-derived  $^{13}\text{C}$  containing isotopologues in TCA cycle are shown as identified by IC-FTMS analysis. The x-axis on the plots is the number of carbons (isotopologues) in the indicated molecule present as  $^{13}\text{C}$  derived from glucose. LSK and MEP cells were collected and pooled from 9-12 mice of matching genotype and considered as one replicate. Data are from two independent experiments. (B) Bar graphs depicting the levels ( $\mu\text{moles per gram protein}$ ) of glucose-derived  $^{13}\text{C}$  containing isotopologues in nucleotides are shown as identified by IC-FTMS analysis. The x-axis on the plots is the number of carbons (isotopologues) in the indicated molecule present as  $^{13}\text{C}$  derived from glucose. Data are from two independent experiments. (C) Expression levels of enzymes involved in the pentose phosphate pathway and nucleotide synthesis pathway in bone marrow MEP cells as determined by RNA sequencing. Data shown is normalized expression levels in *VF* and *E12* versus wildtype cells ( $n=3$  per genotype). All data are presented as mean  $\pm$  SEM. One-way ANOVA analyses followed by Tukey's multiple comparison tests were used for multiple group comparisons (C). \* $P < .05$ ; \*\* $P < .01$ .

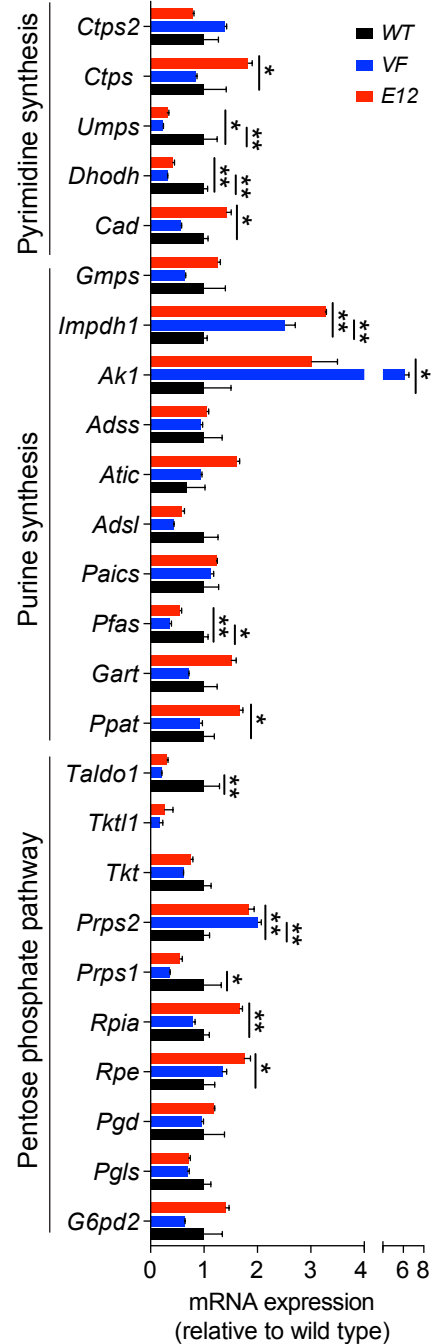
**A** IC-TFMS based tracing of  $^{13}\text{C}$  from labelled  $\text{U-}^{13}\text{C}_6$  D-glucose in LSK and MEP cells



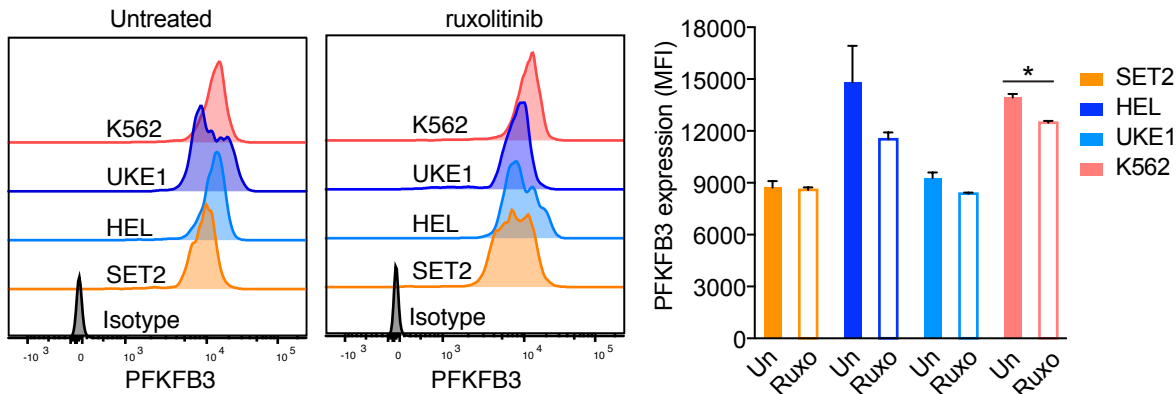
**B** IC-TFMS based tracing of incorporated  $^{13}\text{C}$  from  $\text{U-}^{13}\text{C}_6$  D-glucose in purine/ pyrimidine pathway metabolites in LSK and MEP cells



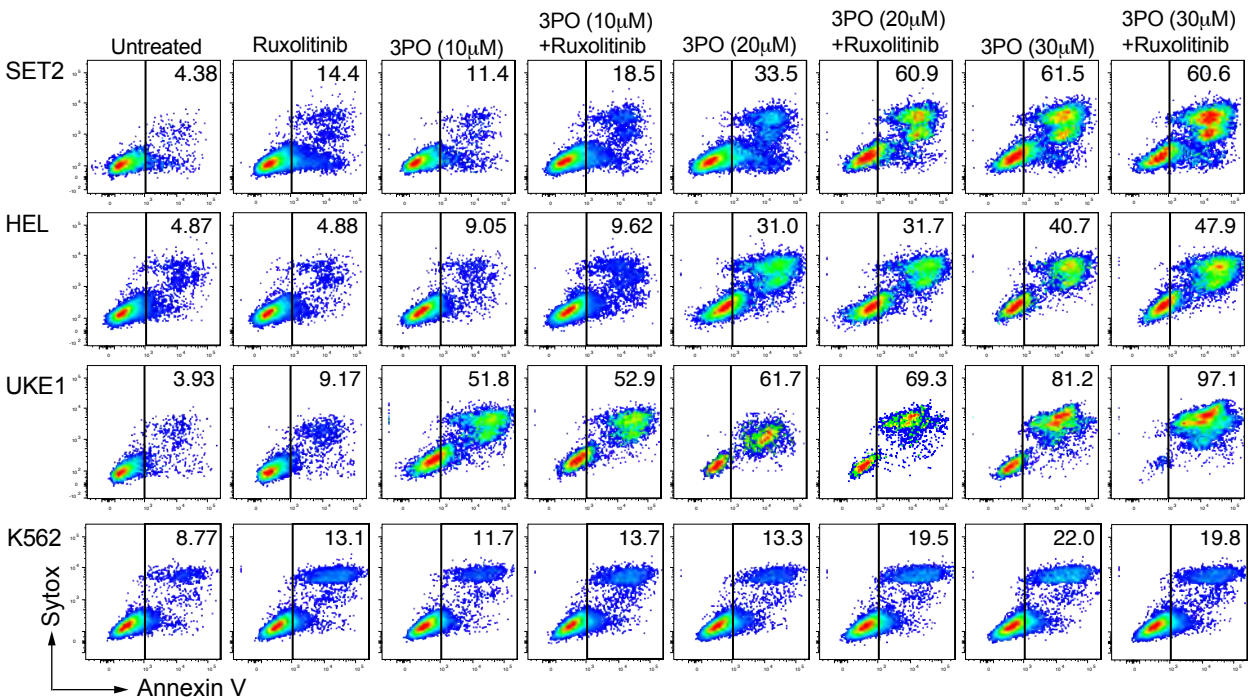
**C** Expression levels of PPP and nucleotide synthesis pathway genes in bone marrow MEP cells



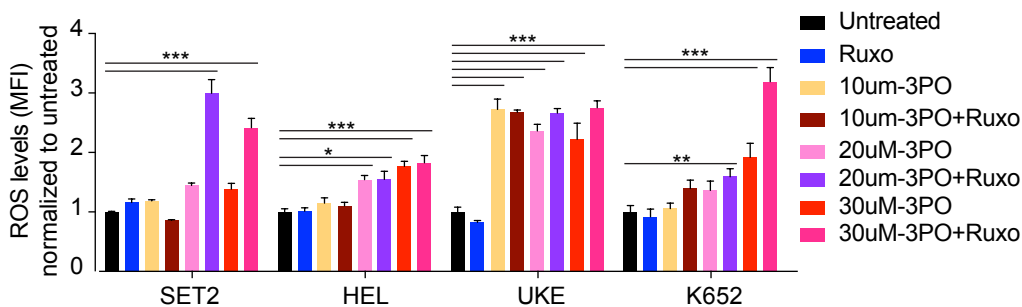
**A** PFKFB3 protein expression in human myeloid leukemia cells



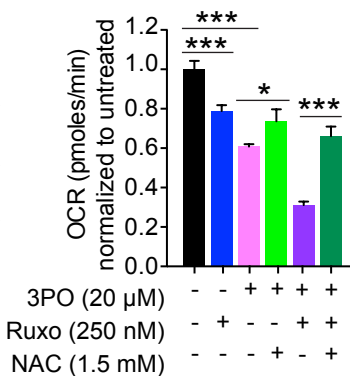
**B** Cell survival rate of human myeloid leukemia cells



**C** Reactive oxygen species (ROS) levels 6 hours after treatment



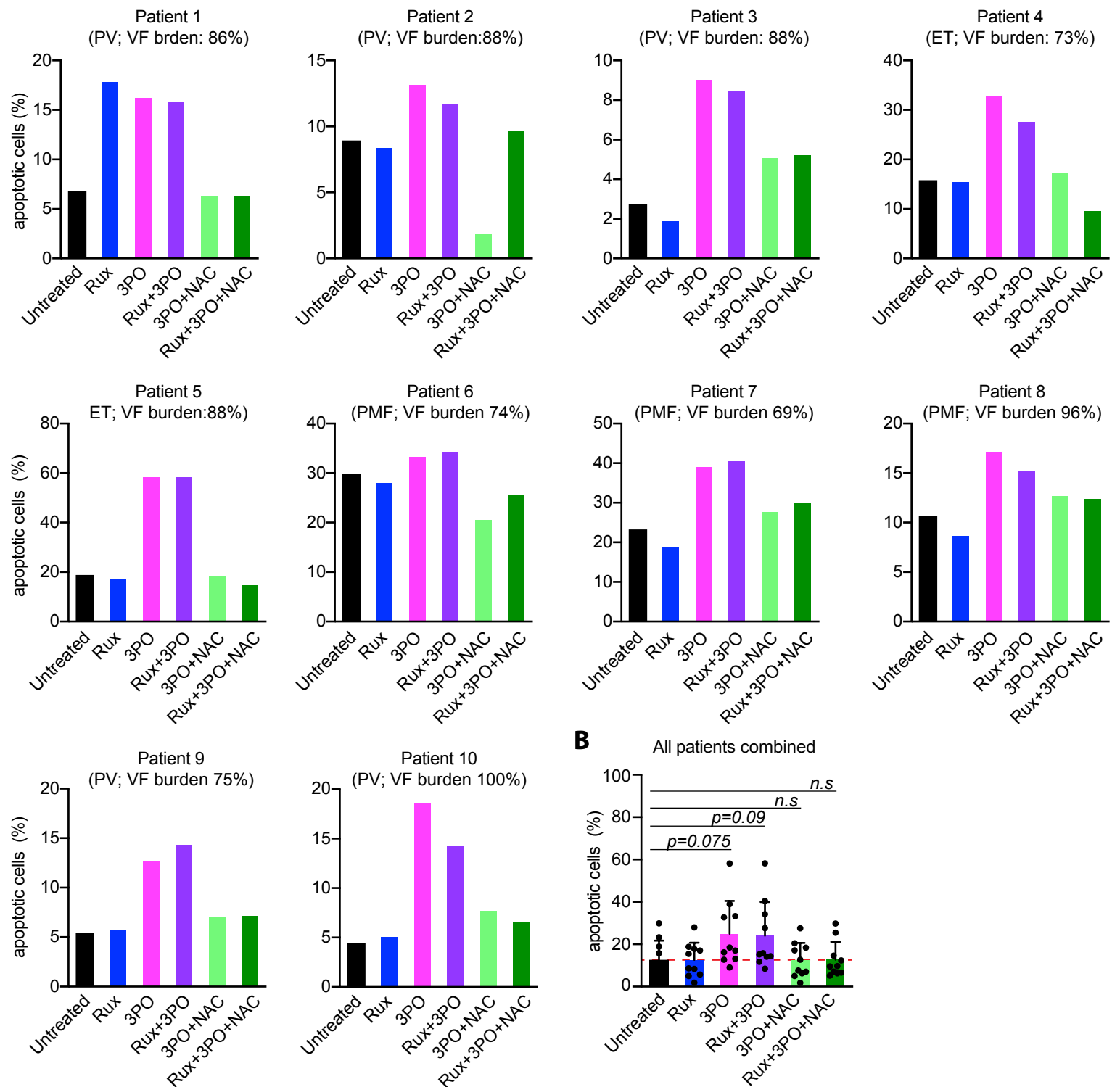
**D** Basal mitochondrial oxygen consumption rate in SET2 cells



**Supplemental Figure S6.** Dual treatment with 3PO and ruxolitinib induces cell proliferation arrest and apoptosis in human leukemic cell lines by evoking ROS levels. (A) Pfkfb3 protein expression in human myeloid leukemia cells (SET2, HEL UKE1, and K562) as determined by flow cytometry after vehicle or ruxolitinib treatment for 24h and shown as representative histogram and bar chart. (B) Representative FACS plots showing the percentages of apoptotic cells after drug treatment for 48 hours (n=3). (C) Bar graph showing the ROS levels in indicated cells treated with 3PO and/or ruxolitinib for 6 hours. Data shown are normalized values of MFI (n=3). (D) Bar graph showing basal OCR levels in indicated cells treated with 3PO and/or ruxolitinib for 6 hours. Cells were pretreated with NAC for 6 hours where indicated. Data shown are normalized values of MFI (n=3 experiments). All data are presented as mean ± SEM. Unpaired Student's t tests (A) or One-way ANOVA analyses followed by Tukey's multiple comparison tests were used for multiple group comparisons (C). \*P < .05; \*\*P < .01; \*\*\*P < .001.

## Supplemental Figure S7

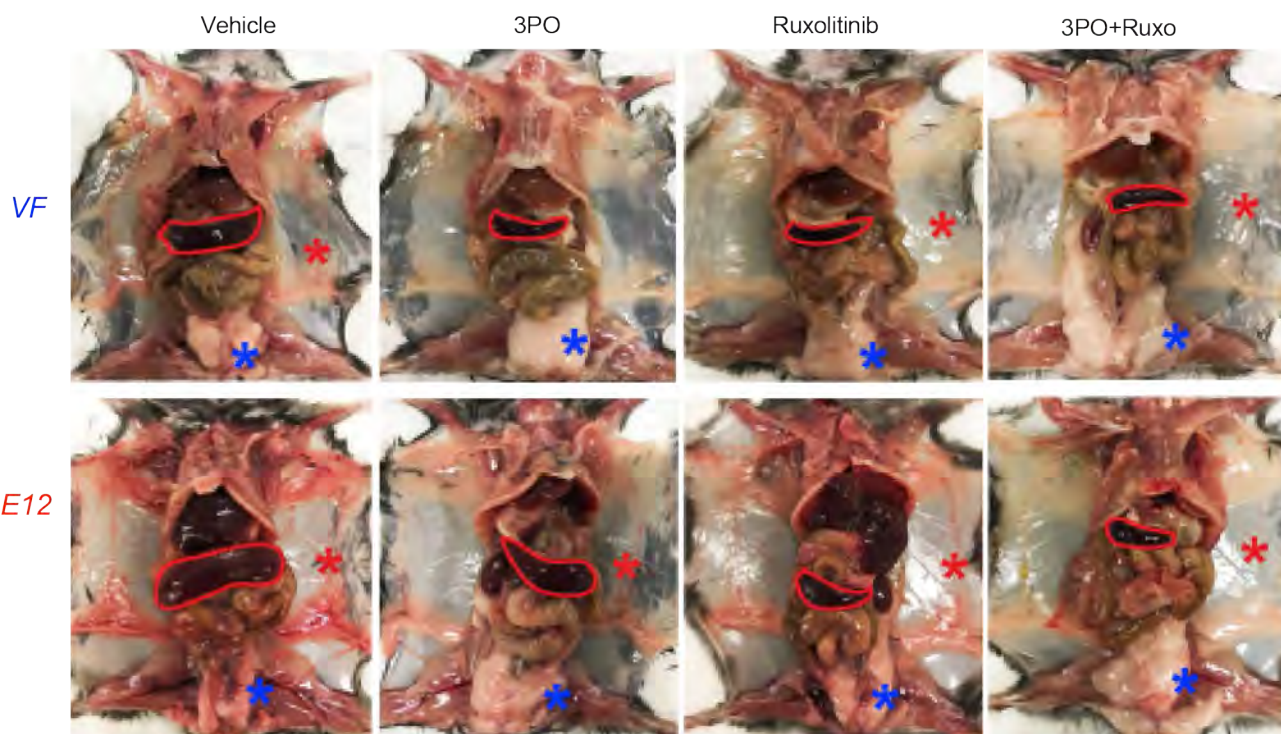
### A Effects of 3PO and Ruxolitinib on survival of PBMC cells from MPN patients



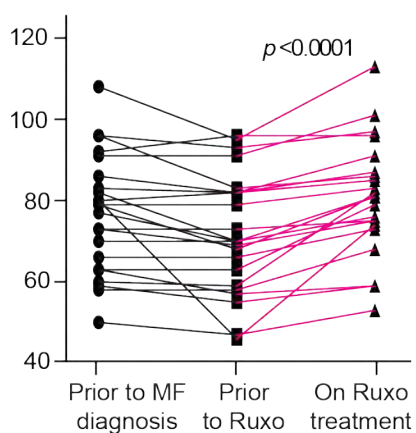
**Supplemental Figure S7.** Inhibition of glycolysis with Pfkfb3 inhibitor 3PO induces apoptosis in peripheral blood mononuclear cells (PBMCs) from MPN patients (n=10). A) Bar graphs show the percentages of apoptotic cells (Annexin V+ Sytox+) in PBMCs treated with 3PO (30 $\mu$ M) or Ruxolitinib (250nM) alone, or in combination for 48hours. PBMCs were pretreated with N-Acetyl-Cystein (NAC) (1.5 mM) for 6 hours where indicated. The MPN subtype and the JAK2-V617F (VF) allele burden (%) of each MPN patients are indicated in parenthesis. B) Plot showing the data of all patient samples combined. Data are presented as mean  $\pm$  SD. One-way ANOVA followed by Tukey's multiple comparison tests were used. n.s.: not significant.

# Supplemental Figure S8

## A Effects of 3PO and ruxolitinib treatment on spleen size and adipose tissue



## B Effect of Ruxolitinib treatment on body weight (kg) in MPN patients



**Supplemental Figure S8.** Combined inhibition of Pfkfb3 activity and hyperactive JAK2 signaling ameliorates adipose atrophy in MPN mice. (A) Representative pictures of mice treated with indicated drugs for 8 weeks.

Red and blue asterisks indicate subcutaneous and epididymal white adipose tissue (eWAT), respectively

(n=6 mice per genotype and treatment). (B) Body weight changes in MPN patients prior to diagnosis, prior to- and

during Ruxolitinib treatment. One-way ANOVA followed by Tukey's multiple comparison tests were used.